International Journal of Thermophysics, Vol. 14, No. 4, 1993

Application of the Taylor Dispersion Method in Supercritical Fluids[1]

J. M. H. Levelt Sengers,[2] U. K. Deiters,[3] U. Klask,[3] P. Swidersky,[3] and G. M. Schneider[3]

Received February 3, 1993

This paper describes some of the experimental and theoretical problems encountered when the Taylor dispersion method is applied to the measurement of diffusion coefficients near gas–liquid critical points. We have used our own measurements of diffusion of benzene and toluene in supercritical carbon dioxide, along with measurements from several other sources, to illustrate some of the experimental challenges. Special attention is given to the peak shape. The intercomparisons are greatly simplified by comparing the experimental data as functions of density, rather than pressure. We find large and unexplained discrepancies between the various experimental sources. We discuss the theoretical predictions for the relationships between the diffusion coefficients and diffusivities obtained from Taylor dispersion and dynamic light scattering in fluids near critical points. We conclude that there is no strong reason to press for Taylor dispersion measurements near the gas–liquid critical point of the carrier gas.

KEY WORDS: benzene; carbon dioxide; critical behavior; data comparison; diffusion coefficient; diffusivity; peak shape; supercritical fluids; Taylor dispersion; toluene; transport coefficients.

1. INTRODUCTION

In this paper, dedicated to Professor Joseph Kestin, the maestro of viscosity and thermal conductivity measurement, we discuss the determination and critical behavior of another transport coefficient, namely, the

[1] Paper dedicated to Professor Joseph Kestin.

[2] Thermophysics Division, National Institute of Standards and Technology, Gaithersburg, Maryland 20899, U.S.A.

[3] Lehrstuhl für Physikalische Chemie II, Ruhr-Universität Bochum, D-44780 Bochum, Germany.

0195-928X/93/0700-0893$07.00/0

binary diffusion coefficient. Measurements of transport coefficients near critical points of compressible fluids have never been a simple task. There are two principal reasons for this difficulty. First, until the advent of dynamical light scattering, these measurements have required the imposition of a macroscopic gradient in temperature, pressure, or concentration. Because of the divergence of the corresponding susceptibility, such gradients cause increasing disturbance of the system as the critical point is approached and are, therefore, "self-limiting" in the sense that the size of the gradient employed sets a limit to the approach to the critical point. Second, traditionally, such experiments have been carried out as a function of pressure and temperature, without control or measurement of the experimental density. Many are the reports in the literature of anomalies in the transport coefficients of pure fluids that later turned out to be due to experimental artifacts; for a review, see Ref. 1.

A theoretical appreciation and understanding of the nature of the critical anomalies of transport coefficients became possible only after experimental techniques were perfected to the point that reliable results could be obtained near critical points. Thus, the first reliable determination of the presence of a very weak anomaly in the viscosity of a pure fluid near the gas–liquid critical point [2] was possible only after Joseph Kestin and his collaborators perfected the oscillating-disk viscometer to a level of accuracy that made the instrument the world's standard for viscosity measurement. Likewise, the considerably stronger anomaly in the thermal conductivity of gases observed by Sengers and co-workers [3, 4] was established with certainty only after perfection of the parallel-plate thermal conductivity apparatus.

A satisfactory state of knowledge and understanding has been recently attained in the measurement of the binary diffusion coefficient D_{12} by means of light scattering and by means of Taylor dispersion in binary liquids near consolute points [5].

The measurement of diffusion coefficients near gas–liquid critical points, however, has not yet been perfected to the point reached for the other transport coefficients. In applications in the highly compressible regime near the gas–liquid critical point, it has proven hard to obtain reliable data, thus thwarting efforts to enhance the theoretical insight. The recent review of Liong et al. [6] of the various methods used in supercritical fluids is a good example of the state of affairs. Although all experimental methods are described and extensive references to literature data are given, no data comparison or evaluation is made. The various theories that have been proposed for the critical behavior of the diffusion coefficient are summarized, but the connection with the experimental data obtained by tracer methods, light scattering and Taylor dispersion is not made. Only

very recently, in the paper by Clifford and Coleby [7], a realization of the special difficulties in this regime begins to emerge.

In this paper, we discuss the experimental limitations of the Taylor dispersion method in supercritical compressible fluids (a) in principle, (b) on the basis of our own experience, and (c) by comparing the literature data obtained for two key systems, benzene and toluene in supercritical carbon dioxide. In describing our own experiments, we focus on our new results on peak shapes as well as on "self-limitation" effects mentioned above. We carry out the comparison of our own and other literature data by converting all measured pressures to density, thus presenting for the first time a comprehensive data comparison of more than half a dozen sources and complementing the review of Liong et al. We show that the density dependence is inherently simple. We corroborate this finding by a theoretical justification that no critical anomalies are expected in a Taylor dispersion measurement of the diffusion coefficient at infinite dilution near a gas–liquid critical point. We comment on the relation between the infinite-dilution diffusion coefficients obtained from Taylor dispersion and the diffusivities obtained from dynamic light scattering, thus making the qualitatively correct conclusions of Clifford and Coleby more precise.

2. THE TAYLOR DISPERSION METHOD

2.1. General

There is a vast literature on the topic of the Taylor dispersion technique for the measurement of diffusion coefficients. The 1980 paper by Alizadeh, Nieto de Castro, and Wakeham [8] gives a thorough discussion of the method and its application to liquid diffusivity measurements, refers to many of the relevant preceding papers, and investigates the principal sources of error. We therefore limit ourselves to a short summary here, but with the perspective of application to supercritical fluids.

In the Taylor dispersion method, a carrier fluid or fluid mixture flows in laminar steady-state flow through a tube of uniform diameter. A very small amount (a "plug") of a second fluid (a pure compound or a solution) is injected into the carrier fluid. If mutual diffusion were negligible, the plug would assume the Poiseuille profile, elements near the wall remaining stagnant and elements near the center moving on streamlines with up to twice the average velocity. A detector further down the tube would record a widely dispersed peak. On the other hand, if the mutual diffusion coefficient were very large, each element of the injected plug would sample all different streamlines in a short time, and therefore all elements of the injected peak would move with the average speed. A detector downstream would record

the original sharp peak stream by, except for the broadening caused by diffusion in the axial direction, which, in our application, is always a small effect. Thus, the broadening of the injected peak is a measure of the mutual diffusion coefficient, a broad peak indicating a low diffusion coefficient.

2.2. Relation of Dispersion and Diffusion Coefficient

We follow the review of Alizadeh et al. [8], centering on issues of importance in our own experiments. The original calculation of the relation between the peak width and the diffusion coefficient was due to Taylor [9]. He showed that at infinite tube length, the peak becomes Gaussian. Aris [10] corrected some of the assumptions made by Taylor and calculated the moments of the axial distribution in an infinitely long tube in terms of the physical parameters of the tube and of the diffusion coefficient. For definitions of the moments, we refer to Aris' paper. The cross-section averaged normalized second spatial moment μ_2' was given by Aris [10] as

$$\mu_2' = 2\left(D_{12} + \frac{\bar{u}_0^2 a_0^2}{48 D_{12}}\right) t - 128 \frac{\bar{u}_0^2 a_0^4}{D_{12}^2} \sum \alpha_{0n}^{-8} \left[1 - \exp\left(-\frac{\alpha_{0n}^2 D_{12} t}{a_0^2}\right)\right] \quad (1)$$

Here D_{12} is the mutual diffusion coefficient, $\bar{u}_0$ the average velocity, a_0 the radius of the tube, and t the time; the α_{0n} are known numerical coefficients. The second term on the right-hand side includes a transient. In our application, typical values of experimental parameters are as follows: flow speed $\bar{u}_0 = 0.5\ \text{cm} \cdot \text{s}^{-1}$; capillary radius $a_0 = 0.04$ cm; duration of an experiment $t = 7200$ s; binary diffusion coefficient $D_{12} = 10^{-4}\ \text{cm}^2 \cdot \text{s}^{-1}$; capillary length $L = 40$ m; coil radius $R_c = 10$ cm;[4] injection volume, 0.5 μl; detector volume $V_D = 0.25\ \mu$l; and typical standard deviation of peak when detected, 60 s (30 cm).

In our case, the product $D_{12} t / a_0^2$ is very large, since the time required to reach the detector is of the order of 2 h, and therefore the second term on the right-hand side is reduced to a constant. Furthermore, the entire second term is a very small fraction (approximately 10^{-4}) of the first and can be neglected. We therefore calculate the diffusion coefficient from the relation

$$\mu_2' \approx 2\left(D_{12} + \frac{\bar{u}_0^2 a_0^2}{48 D_{12}}\right) t \quad (2)$$

[4] The capillary was arranged as an oval, with half of its length being straight (2 semicircular sections, curvature radius R_c, 30 cm apart).

The value for a_0 is the radius of the tube, not the diameter, as erroneously stated (but correctly used) in Ref. 11. In our application, the term inversely proportional to D_{12} dominates, but the term linear in D_{12} is not quite negligible (800 times smaller), so we include it in our evaluation of the diffusion coefficient from the measured second moment.

If an infinitely narrow peak is injected, the peak will become a Gaussian only at infinite time. For any finite time the peak is expected to display a skewness S, the ratio of the square of the third moment to the cube of the second moment, given by [8, 10]

$$S = \frac{(\mu_3')^2}{(\mu_2')^3} = \frac{49\bar{u}_0^6 a_0^8}{2^{20} D_{12}^7 \left(1 + \dfrac{\bar{u}_0^2 a_0^2}{48 D_{12}^2}\right)^3 t} \tag{3}$$

For the experimental parameters listed above, we calculate the skewness to be expected for our experiments from this effect to be of the order of $S = 1.2 \times 10^{-2}$. We were unable to reproduce the value $S \approx 10^{-8}$ quoted in Ref. 8.

Alizadeh et al. calculate the error introduced by measuring the temporal distribution at a fixed point in the tube, instead of the spatial distribution at a fixed time. They assume a normal spatial distribution (which is of course not quite true in our case, given the 1% skewness) and then show that, in lowest approximation, the first moment of the temporal distribution (the retention time) differs from that of the spatial distribution by a factor of $(1 + 2\zeta_0)\bar{u}_0^{-1}$, and the second moment of the temporal distribution differs from that of the spatial distribution by a factor of $(1 + 6\zeta_0)\bar{u}_0^{-2}$, with ζ_0 defined as

$$\zeta_0 = \frac{\bar{u}_0 a_0^2}{48 L D_{12}} \tag{4}$$

In our case, this parameter amounts to only 10^{-4}, and therefore the temporal first and second moments can be assumed to be related to the spatial ones by $\mu_i = \mu_i' \bar{u}_0^{-i}$. The temporal moments μ_i are the ones we derive from our experiment.

We have calculated what the effect of replacing the spatial by the temporal peak would have on the third moment and, therefore, on the skewness. We find that this results in a positive contribution to μ_3, which leads to a skewness of approximately 6.5×10^{-4}, somewhat smaller than, but not negligible to, the skewness resulting from finite tube length [Eq. (3)] and that experimentally observed.

Alizadeh et al. also discuss the effect of the detector. If it is assumed that in the transition to the detector (an UV absorption cell), the fluid

element becomes completely mixed, then a new boundary condition is imposed on the diffusion equation at the exit of the tube. In addition, the finite size of the volume induces another correction to the moments due to decreased spatial resolution. The correction to μ_2 due to the changed boundary condition is again proportional to ζ_0, which is negligible in our case. The correction $\delta\mu_2$ for the finite size of the detector volume is given by

$$\delta\mu_2 \propto \left(\frac{L}{\bar{u}_0}\right)^2 \left(\frac{V_D}{\pi a_0^2 L}\right)^2 \tag{5}$$

In our case, V_D is entirely negligible with respect to the volume of the tube, and therefore this correction is of no importance. Similarly, the effect of the finite injector volume on μ_3 and therefore on the peak shape was found to be negligible for our apparatus.

2.3. Determination of the Moments

The instrument at Ruhr-Universität Bochum uses a UV detector to determine the temporal shape of the dispersing UV-active injected species. In previous work, the peak was recorded graphically and analyzed for the location of the maximum and for its width by a tangent construction. Recently, the instrument has been modified by interfacing the UV detector with a computer. Data are presently taken at intervals of a few seconds over the full length of a typical run (five or six peaks, at 13- to 15-min intervals) and permanently stored.

The simplest form of data analysis is a direct calculation of the moments from the following expressions:

$$\begin{aligned}
&v_0 = \sum y_i, && \mu_0 = \frac{1}{v_0}\sum y_i = 1 \\
&v_1 = \sum y_i t_i, && \mu_1 = \frac{1}{v_0}\sum y_i (t_i - \bar{t}) = \frac{v_1}{v_0} - \bar{t} = 0 \\
&v_2 = \sum y_i t_i^2, && \mu_2 = \frac{1}{v_0}\sum y_i (t_i - \bar{t})^2 = \frac{v_2}{v_0} - \frac{v_1^2}{v_0^2} = \sigma^2 \\
&v_3 = \sum y_i t_i^3, && \mu_3 = \frac{1}{v_0}\sum y_i (t_i - \bar{t})^3 = \frac{v_3}{v_0} - 3\frac{v_2 v_1}{v_0^2} + 2\frac{v_1^3}{v_0^3} \\
&v_4 = \sum y_i t_i^4, && \mu_4 = \frac{1}{v_0}\sum y_i (t_i - \bar{t})^4 = \frac{v_4}{v_0} - 4\frac{v_3 v_1}{v_0^2} + 6\frac{v_2 v_1^2}{v_0^3} - 3\frac{v_1^4}{v_0^4} \\
&\vdots && \vdots
\end{aligned} \tag{6}$$

Here the v_i are temporal moments with respect to a starting point preceding in time (t) the beginning of the peak, and the y_i are the UV detector readings relative to a background term which is linearly interpolated between a point just before and just after the peak. The μ_i are temporal moments normalized with respect to the center of the peak. By varying the beginning and end point of the calculation within a reasonable range, we find that the normalized second moment μ_2 is stable on the level of a few tenths of a percent.

Alternative ways of analyzing the data have been explored: After subtraction of the background, as explained earlier, the data have been fitted to a Gaussian by linear regression, which requires the taking of a logarithm and appropriate adjustment of the weights. Furthermore, a direct fit of the experimental data to a skewed Gaussian with a linear background function has been done by nonlinear regression, by means of the Marquardt–Levenberg algorithm.

The results of the calculation of moments by these three different procedures are summarized in Table I for six sample peaks, arbitrarily chosen from our collection of data for benzene and toluene in CO_2, discussed later. In the worst case, labeled No. 15, the second moments from the three analyses have a spread of 7%. In all other cases, the spread is under 6%. In the diffusion coefficients we report, we select for each peak the one of the three different methods of calculation which gives the best deviation plot, then average over the number of peaks measured for the particular state point.

The results of the moment summation are the most revealing, because

Table I. Evaluation of Standard Deviations or Moments from Experimental Peak Shape[a]

	Linearization	Nonlinear regression	Momentum summation				
No.[b]	σ^2 (s^2)	σ^2 (s^2)	μ_2 (s^2)	μ_3 (s^3)	μ_4 ($10^7 s^4$)	$3\mu_2^2$ ($10^7 s^4$)	S
4	3,461	3,531	3,450	8,260	3.457	3.571	1.66×10^{-3}
8	3,346	3,519	3,308	2,713	3.080	3.283	0.20×10^{-3}
14	3,312	3,415	3,298	12,400	3.198	3.263	4.28×10^{-3}
14	3,316	3,576	3,310	−9,201	3.272	3.287	2.33×10^{-3}
15	3,737	4,003	3,729	21,297	4.195	4.172	8.75×10^{-3}
17	3,531	3,454	3,493	17,178	3.668	3.660	6.92×10^{-3}

[a] Linearization: weighted linear regression of logarithmic plot. Nonlinear regression: fit to a skewed Gaussian by means of a Marquardt–Levenberg algorithm. Momentum summation: according to Eq. (6). σ, standard deviation in seconds, (s); μ_i, moments Eq. (6); S, skewness, Eq. (3).

[b] The numbers refer to experimental conditions listed in Tables V and VI.

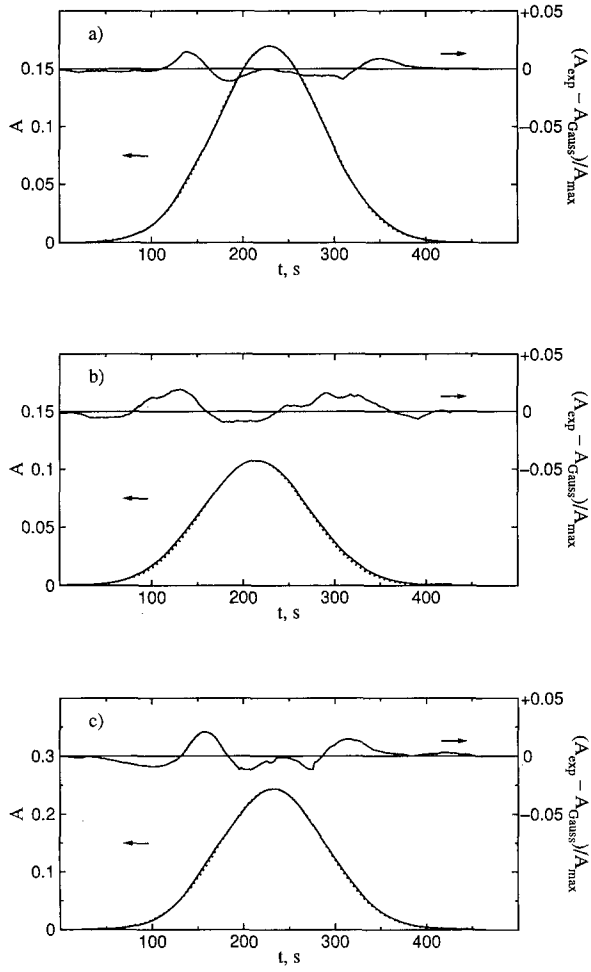

Fig. 1. Detector output of a Taylor dispersion experiment (UV absorbance A; left scale). (——) Experimental data; (·····) pure Gaussian, as determined from the second moment of the experimental data. The upper portion of the diagrams shows an enlarged deviation plot $[(A_{exp} - A_{Gauss})/A_{max}$; right scale]. (a, b) Benzene in CO_2 (experimental conditions; see entries 4 and 8 in Table V); (c) toluene in CO_2 (entry 14 in Table VI).

they permit a check on the Gaussian character of the peak shape. For a true Gaussian, the third moment μ_3 and the peak skewness S are zero, and the fourth moment equals three times the square of the second. From the data in Table I it is clear that the third moment is relatively small and almost always positive, and that the peak skewness S is between 0.1 and 1%, as expected for our apparatus conditions. Also, we find that the Gaussian condition $\mu_4 = 3\mu_2^2$ is fulfilled on the level of a few percent.

In Figs. 1a–c, we display some of the measured absorbance peaks, curves a and b being for benzene in CO_2, and curve c for toluene in CO_2. The lower part of each diagram shows the measured peak (full curve) and the pure Gaussian based on the second moment derived from the data (dotted curve). It is seen that the departures from a pure Gaussian are no more than a few percent. Nevertheless, the three peaks have some systematics in common: The top of the measured peak is slightly low, while the wings "bulge." This systematic effect is seen in many of our fitted peaks and may be due to spurious "peak averaging" caused by fluctuations in the expansion section of the apparatus (see Section 3.5) or to other potential artifacts, such as nonlinearity of the detector. On the other hand, there seldom is any indication of "tailing" or other peak asymmetry beyond what is to be expected.

2.4. Tube Coiling

Traditionally, Taylor dispersion is measured in long tubes that need to be coiled in order to keep their temperature homogeneous. Alizadeh et al. [8] discuss the disturbance of the Poiseuille flow in a coiled tube, referring to earlier fundamental studies by Janssen [12] and by Nunge et al. [13]. Nunge et al. point out that tube coiling has two effects. First, the velocity profile is elongated, leading to greater dispersion of the peak and smaller apparent values of D_{12}. Second, centrifugal effects set up secondary flow perpendicular to the flow direction and, therefore, increase the mixing, thus augmenting the diffusional effects; this leads to narrower peaks and larger apparent values of D_{12}. Janssen treats only the second effect. Alizadeh et al. quote the full expression from Nunge, but with the opposite sign for the effect on the second moment.

The dimensionless parameter characterizing the curvature of the coil is

$$\omega = \frac{R_c}{a_0} \tag{7}$$

which in these applications is always large, in our case about 250. In that case, according to Alizadeh et al., the correction to the second moment due

to the tube curvature depends on the dimensionless group De^2Sc, where De is the Dean number,

$$De = Re\,\omega^{1/2} \tag{8}$$

Re is the Reynolds number,

$$Re = \frac{2a_0\bar{u}_0\rho}{\eta} \tag{9}$$

with ρ the mass density and η the viscosity, and Sc is the Schmidt number,

$$Sc = \frac{\eta}{\rho D_{12}} \tag{10}$$

The relative sizes of the two effects are discussed in some detail in the paper by Nunge et al. [13], who show that the peak broadening effect, due to a term proportional to $Re^2Sc\omega^{-2}$, and therefore not simply dependent on the dimensionless group De^2Sc, dominates at small Reynolds numbers if $\omega \leqslant 10$, while the peak narrowing effect, proportional to $Re^4Sc^2\omega^{-2} = (De^2Sc)^2$, dominates at larger Reynolds numbers. Janssen calculates only the secondary flow effect, mentions that it is proportional to $(De^2Sc)^2$, and states that it decreases the axial dispersion if this parameter exceeds the value of 100. Alizadeh et al. [8], however, though using the full expression for the dispersion coefficient from the Nunge paper (be it with the opposite sign), show only an *increase* in the second moment (their Fig. 4, p. 265, for $\omega \geqslant 100$). The shift in the second moment increases, apparently quadratically, with increasing De^2Sc, to reach about 1% when this dimensionless group exceeds the value of 60. We have assumed that the sign in the Alizadeh paper is incorrect for our application.

In our application, we have the following typical values for the dimensionless numbers and fluid parameters ρ [14] and η [15]: $\rho = 0.7\ g \cdot cm^{-3}$; $\eta = 57\ \mu Pa \cdot s$; $\bar{u}_0 = 0.5\ cm \cdot s^{-1}$; $\omega = 250$; $Re = 50$; $Sc = 10$; and $De = 4$. It follows that De^2Sc is about 160, so that we must expect a nonnegligible decrease in the second moment (apparent increase in D_{12}) due to centrifugal effects (approximately 2.3% for the conditions listed above, according to Eq. (71) in Ref. 8, see Fig. 2). In practice, the effect should be smaller, because our capillary was coiled as an oval, and the ω value given above applies only to half of the length of the capillary. Experimentally, such effects can be tested by measuring the dispersion as a function of flow speed. In the paper by Swaid and Schneider [16], for instance, a marked increase in the apparent diffusion coefficient was noted in an apparatus of similar dimensions at high flow speeds. Even in the speed range of 0.6 to

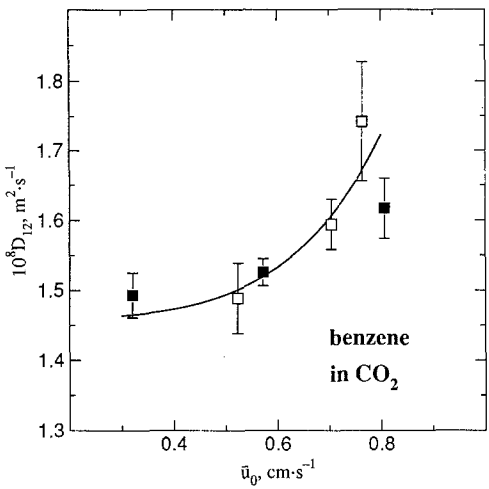

Fig. 2. Influence of flow speed $\bar{u}_0$ on the observed diffusion coefficient. Benzene in CO_2, density $\rho = 0.701$–$0.703\ g \cdot cm^{-3}$. (□) 307.9 K; (■) 309.7 K; (——) calculated from Eq. (71) in Ref. 8 (with the opposite sign of the coiling correction) for experimental conditions and hydrodynamic parameters listed above.

$2.5\ cm \cdot s^{-1}$, the measured diffusion coefficients increase by several percent (Fig. 3 in Ref. 16). Because of this finding, a flow speed of $0.5\ cm \cdot s^{-1}$ has usually been adopted, as a compromise between experimental feasibility and absence of secondary flow effects. It is practically not feasible to decrease our flow speed substantially, since increasing the retention time much beyond the present several hours will increase the effect of uncontrolled disturbances. Nevertheless, we have some indication of flow-speed dependence from our own measurements. In Fig. 2, we show the diffusion coefficient of benzene in CO_2 determined for fixed state conditions of pressure, temperature, and density, measured at flow speeds from 0.3 to $0.8\ cm \cdot s^{-1}$. A trend exceeding the experimental uncertainty is visible, and the sign is consistent with peak narrowing at higher flow speed. It is obvious that this effect could have many causes. Whatever the cause, however, Fig. 2 pinpoints one artifact that may cause our diffusion coefficients to be several percent high if measured at flow speeds exceeding $0.5\ cm \cdot s^{-1}$.

3. HIGHLY COMPRESSIBLE STATES

3.1. Density Variation Due to Limited Pressure and Temperature Control

The diffusion coefficient of a fluid is a function of the fluid density. Any error in the observed pressure and temperature causes an error in the density. Diffusion coefficients are seldom measured to better than 1% uncertainty. If it is assumed that the diffusion coefficient varies roughly inversely to the density, one needs to control the fluid density to somewhat better than 1% for the density uncertainty not to cause appreciable error in the diffusion coefficient.

In Taylor dispersion experiments, typical uncertainties of temperature control and measurement are about 0.1 K, and those of pressure control and measurement about 0.01 MPa. For applications to liquids, this is adequate. For supercritical states, the uncertainty of the density as a consequence of the pressure and temperature uncertainty becomes very large near the critical point of the carrier gas. In Table II, we present some estimates of the density uncertainties caused by the typical 0.1 K and 0.01 MPa uncertainties at various states of supercritical carbon dioxide. The equation of state of Ref. 14 was used to calculate these uncertainties. From the data in Table II we conclude that with this quality of temperature and pressure control, if the density range from 0.3 to 0.6 $g \cdot cm^{-3}$

Table II. Effect of a Temperature Variation $\delta T = 0.1$ K or of a Pressure Variation $\delta P = 0.01$ MPa on the CO_2 Density

T (K)	P (MPa)	ρ ($kg \cdot m^{-3}$)	$(\partial\rho/\partial T)_P \delta T$ ($kg \cdot m^{-3}$)	$(\partial\rho/\partial P)_T \delta P$ ($kg \cdot m^{-3}$)
306	9.0	703	1.7	0.5
	8.5	674	2.3	0.7
	8.0	621	4.4	1.7
	7.5	316	3.4	3.0
	7.0	234	0.8	1.0
310	10.0	686	1.6	0.5
	9.0	615	3.0	1.2
	8.5	515	7.1	3.6
	8.0	327	2.5	2.2
313	13.5	755	0.9	0.2
	12.0	719	1.1	0.3
	10.0	632	2.1	0.7
	9.5	584	3.0	1.2
	9.0	493	4.9	2.6
	8.5	358	2.7	2.1

is entered at temperatures below 310 K (37°C, 6 K above the critical point of CO_2), a density uncertainty is incurred exceeding 1%. This sets a practical limit to the applicability of the Taylor dispersion method in supercritical fluids.

We have recently improved the control and measurement of the temperature of the dispersion tube to 0.01 K. This considerably reduces the uncertainty in the density due to temperature fluctuations of the tube. The uncertainty of the pressure, and several other factors to be discussed, still leaves the region specified above inaccessible to reliable experimentation.

3.2. Disturbances of Laminar Flow Due to Inhomogeneous Density

The analysis of the Taylor dispersion experiment is founded upon the assumption of Poiseuille flow. Necessary conditions are that the fluid properties, in particular the density and the viscosity, are independent of the position in the tube, irrespective of the concentration of the second component. None of these assumptions can be taken for granted in applications near the critical point of the carrier gas. Even in a pure fluid flowing through a tube, there are several reasons that the density is no longer homogeneous. In the axial direction, pressure gradients required to maintain the flow will lead to density gradients driven by the high compressibility κ_T. As the density varies, so does the viscosity. Only very recently, van den Berg, ten Seldam, and van der Gulik [17, 18] have made the first analysis of the disturbance of the parabolic flow profile in the case of a near-critical pure fluid flowing through a cylindrical tube.

Alizadeh et al. [8] discuss some of the consequences of the fact that the density of the injected liquid sample is necessarily different from that of the carrier fluid. Axial density differences will lead to longitudinal pressure gradients that modify the flow. Radial gradients lead to secondary flow driven by buoyant forces. They mention that no satisfactory approximate solutions of the Taylor dispersion process exist even in the case that density gradients are small and linear in concentration. After the second substance is injected, there will be a transient period during which the sharp concentration and density gradients diminish sufficiently that the ordinary Taylor dispersion process can take over, but a mathematical analysis of the transient process is not available.

Alizadeh et al. therefore advise keeping the concentration differences as small as possible, by adjusting the composition of the injected peak close to that of the carrier fluid. In the case of binary liquid mixtures near consolute points, this technique has proven very effective, as discussed in a recent publication by Matos Lopes et al. [5]. Alizadeh et al. state that

ultimately, however, the only means to be sure that no buoyancy effects are present is to show that the diffusion coefficient obtained is independent of flow velocities and injection concentrations.

3.3. Solute Effects on Density Near the Solvent Critical Point

The difficulties discussed in Section 3.2 are greatly magnified if the process of Taylor dispersion is applied near a gas–liquid critical point. The very fact of injecting a spike of different composition into a near-critical fluid leads to a significant change of the density, again driven by the high compressibility. A recent paper by Clifford and Coleby [7] draws attention to this problem in the application to naphthalene diffusing into supercritical carbon dioxide as a carrier; that paper presents estimates of the density disturbance due to the injection, based on a van der Waals-type mixture equation of state. The authors find that even 9 K above the critical point of CO_2, the density may increase by several percent when 0.04 mol% of naphthalene is present in CO_2.

We have found it more convenient to estimate the effect on the basis of dilute-mixture thermodynamics as developed by Levelt Sengers and co-workers [19, 20], with pure carbon dioxide as the reference system. By using the relation $(\partial\rho/\partial x)_{P,T}(\partial x/\partial P)_{\rho,T}(\partial P/\partial\rho)_{x,T} = -1$, we find, for the density variation $\delta\rho$ due to a composition variation δx $(=x)$ at fixed pressure and temperature,

$$\delta\rho = -x\left(\frac{\partial P}{\partial x}\right)^{c}_{\rho,T}\left(\frac{\partial\rho}{\partial P}\right)_{T,x} \tag{11}$$

Here it is assumed that the distance from the critical point is large enough that the density shift is still linear in the mole fraction x, and the mole fraction is small enough that the compressibility of the pure carrier gas [14] can be used (for departures from these conditions, see Refs. 19 and 20). The derivative $(\partial P/\partial x)_{\rho,T}$ has no strong critical anomalies, and therefore its critical value, indicated by the superscript c, can be used as a first approximation in the vicinity of the solvent's critical point. This value is obtained from the initial slope of the critical line or from the common slope of dew and bubble point line at the solvent's critical point [19, 20].

In Table III, some typical values of the density change of carbon dioxide due to the presence of a mole fraction of toluene of 0.01 are given, based on the approximate relation (11), a value of -20 MPa obtained for $(\partial P/\partial x)_{\rho,T}$ from the initial slope of the near-critical dew-bubble curves for toluene in CO_2 [21] and the equation of state of CO_2 [14]. Consistent with the findings of Clifford and Coleby (but with far less work), we find,

Table III. Effect of a Toluene Mole Fraction of 0.01 on the CO_2 Density

T (K)	P (MPa)	ρ ($kg \cdot m^{-3}$)	$(\partial\rho/\partial P)_T$ ($kg \cdot m^{-3} \cdot MPa^{-1}$)	$\delta\rho$ ($kg \cdot m^{-3}$)
310	10.0	686	47	9
	9.0	615	115	23
	8.5	515	363	72
	8.0	327	221	44
313	13.5	755	20	4
	12.0	719	28	6
	10.0	632	74	15
	9.5	584	123	25
	9.0	493	261	52
	8.5	358	214	42
333	15.0	605	37	7
	12.0	436	77	15
	9.0	236	49	10

6 K above the critical point, a maximum density increase of 15% for a toluene mole fraction of 0.01.

In order to appreciate the departures from the condition of constant density in the vicinity of the peak, we need to know something about the range of concentrations sampled in our experiment. If 0.2 μl of sample is injected, the spike is 0.04 cm long. At the tube exit, the peak is about 1 m long. If the sample injected were pure toluene, even at the tube exit the mean concentration would still be of the order of 4 parts in 10^4. From the (crudely) estimated density shifts in Table III, it is obvious that for densities within a factor of two from the critical densities and for temperatures as far away as 333 K, 29 K above the critical point of CO_2, the condition of constant density is substantially violated throughout the dispersion tube.

An obvious way to make this problem less acute is to inject the solute already predissolved in the solvent [5, 8, 22–26]. We have recently added a loop before the injection valve, in which we load about 10% of the total volume with solute. We then pressurize the loop to a pressure somewhat below the lowest pressure desired in the experiment (to prevent leakage into the tube through the seals of the injection valve) and let the material homogenize overnight. We can use the material in the loop for many injections, but the material per injection, and therefore the peak size, will slowly decrease during this time.

The density gradients induced by the solute will lead to increased secondary flow when the tube is curved. There will also be disturbances of the Poiseuille flow due to the fact that the viscosity varies along with the density. As a consequence, the more viscous material will tend to remain

closer to the axis. When a second component is present, a concentration gradient may be induced which counteracts the Taylor dispersion process. To our knowledge, no mathematical analysis exists of this effect.

In conclusion, the density change induced by the solute in the near-critical carrier gas is substantial and leads to numerous problems in the interpretation of the Taylor dispersion experiment.

Moreover, as long as there is no solution of the Taylor dispersion problem for compressible flow, the diffusion coefficient values obtained from measurements in supercritical fluids can be trusted only if they have been shown to be independent of fluid flow speed. In addition, the solute needs to be prediluted in the solvent, and it needs to be demonstrated that the diffusion coefficient is measured in a regime where the value is independent of the initial concentration.

3.4. Density Gradients Due to Pressure Gradients

The nearness to a critical point will amplify the density gradients that exist because of the necessary pressure gradient inducing the flow. In our experiment, the pressure difference across the tube for typical conditions (see Section 2.2) is about 600 Pa, or 6 mbar. When the fluid is not compressible, this effect, barely 1 part in 10^4 of the total pressure, is irrelevant. In fact, it is smaller than the pressure resolution of our manometer, approximately 0.015 MPa. In a supercritical fluid, however, it could be significant. In Table IV, we show the approximate difference in density at the beginning and the end of the tube due to this pressure difference. At a distance of 6 K above the critical point, the density variation is less than 1 part in 2000 in our experiment and, therefore, not a source of significant error.

3.5. Density Variations Due to Temperature Variations

A typical Taylor dispersion apparatus contains, in addition to a temperature-controlled dispersion tube, a detector and an expansion section.

Table IV. Density Difference Along the Tube

T (K)	P (MPa)	ρ (kg·m^{-3})	$(\partial\rho/\partial P)_T$ (kg·m^{-3}·MPa^{-1})	$\delta\rho$ (kg·m^{-3})
310	10.0	686	47	0.03
310	9.0	615	115	0.07
310	8.5	515	363	0.22
310	8.0	327	221	0.13

In our case, the cell of the UV detector has a very small volume (less than 1 μl) and is temperature-controlled by thermostated flowing water. The expansion section consists of a pressure regulator followed by a needle valve. Since there is considerable cooling associated with the expansion of the carrier fluid, the expansion section is located in a separate air thermostat with on–off temperature control on the level of a few tenths of a kelvin (a liquid thermostat is under construction). The volume of the carrier gas in this air thermostat, prior to expansion, is not small, and pressure variations due to the alternating temperature can feed back to the preceding dispersion tube. As a consequence, a peak passing through the detector will move back and forth, thus affecting the shape registered by the detector. We believe that this may be one reason that the maxima of our peaks are somewhat low, or the wings slightly high, compared to a true Gaussian, detector nonlinearity being another possibility. At temperatures of 313 K and lower, in practice measurement became irreproducible for densities lower than 0.7 $g \cdot cm^{-3}$.

4. DIFFUSION COEFFICIENTS FOR BENZENE AND TOLUENE IN CARBON DIOXIDE

4.1. Data Obtained at Ruhr-Universität Bochum

At various times, experimental data for the diffusion coefficients of benzene and toluene have been obtained in forerunners of the present apparatus. For details about the apparatus, we refer to Refs. [25–30]. Some of these data are tabulated or graphically presented in the archival literature [16, 25, 27], but other data are available only in Diploma theses [28–30].

We begin by summarizing the new data we have obtained with the apparatus in the past year, after computerizing the data recording and processing, installing a new UV detector and a sample dilution loop, and improving temperature control and measurement.

The diffusion coefficients for benzene are summarized in Table V, and those for toluene in Table VI. In most cases, five samples were injected at 13-minute intervals. For each peak, a second moment is calculated in several ways, as explained before, and a diffusion coefficient calculated from the average second moment by means of Eq. (2). The uncertainty of the diffusion coefficients quoted in Tables V and VI is one standard deviation based on the distribution of values for the five peaks.

The temperature is recorded on five sensors distributed along the coiled tube, and the uncertainty quoted is one standard deviation based on these five readings, time-averaged over the duration of the experiment. The

Table V. Diffusion Coefficient of Benzene in Carbon Dioxide

No.	T (K)	ρ ($g \cdot cm^{-3}$)	$10^4 D_{12}$ ($cm^2 \cdot s^{-1}$)	$\bar{u}_0$ ($cm \cdot s^{-1}$)	P (MPa)[a]
1	314.14 ± 0.07	0.6068 ± 0.0030	1.98 ± 0.06	0.6418 ± 0.001	10.00
2	314.14 ± 0.07	0.7451 ± 0.0009	1.51 ± 0.03	0.7907 ± 0.004	13.53
3	307.94 ± 0.02	0.7030 ± 0.0009	1.49 ± 0.05	0.5228 ± 0.001	9.68
4	307.93 ± 0.01	0.7779 ± 0.0004	1.37 ± 0.02	0.6466 ± 0.001	12.46
5	307.93 ± 0.02	0.7031 ± 0.0009	1.59 ± 0.04	0.7044 ± 0.001	9.68
6	307.92 ± 0.02	0.7032 ± 0.0010	1.74 ± 0.09	0.7632 ± 0.001	9.68
7	309.67 ± 0.03	0.7010 ± 0.0010	1.62 ± 0.04	0.8065 ± 0.001	10.24
8	309.68 ± 0.03	0.7009 ± 0.0010	1.53 ± 0.02	0.5712 ± 0.001	10.24
9	309.66 ± 0.02	0.7015 ± 0.0008	1.49 ± 0.03	0.3204 ± 0.001	10.25

[a] Pressure uncertainty, ± 0.015 MPa.

density is calculated from the pressure, read on a high-quality Heise gauge, and the temperature, by means of an equation of state of Span and Wagner [14]. The uncertainty in the density is based on a propagation-of-error calculation in which it is assumed that the pressure uncertainty is 0.015 MPa, and the temperature uncertainty is the one listed. For each peak, a value of the flow speed is calculated from the residence time and the known length of the tube. The uncertainty listed for the flow speed is one standard deviation, based on the distribution of speeds obtained for the five peaks of each run.

For any individual run of five peaks, the standard deviation is a few percent or less. There is, however, considerably more spread between data obtained in different runs, even at almost-identical pressures and temperatures. At the higher densities, such as the three toluene runs near $0.8\ g \cdot cm^{-3}$ and 307 K (Nos. 11, 16, and 17), the total spread is still within

Table VI. Diffusion Coefficient of Toluene in Carbon Dioxide

No.	T (K)	ρ ($g \cdot cm^{-3}$)	$10^4 D_{12}$ ($cm^2 \cdot s^{-1}$)	$\bar{u}_0$ ($cm \cdot s^{-1}$)	P (MPa)[a]
10	313.73 ± 0.07	0.7491 ± 0.0009	1.42 ± 0.01	0.7432 ± 0.002	13.52
11	306.76 ± 0.02	0.8028 ± 0.0004	1.23 ± 0.02	0.5103 ± 0.002	13.40
12	306.78 ± 0.02	0.7489 ± 0.0006	1.41 ± 0.06	0.5554 ± 0.004	10.63
13	306.12 ± 0.02	0.7492 ± 0.0006	1.44 ± 0.03	0.5592 ± 0.002	10.37
14	308.36 ± 0.27	0.7230 ± 0.0039	1.45 ± 0.02	0.6298 ± 0.003	10.37
15	307.93 ± 0.05	0.7031 ± 0.0016	1.51 ± 0.03	0.5572 ± 0.001	9.68
16	307.90 ± 0.01	0.7946 ± 0.0003	1.29 ± 0.02	0.5044 ± 0.001	13.43
17	307.91 ± 0.01	0.7946 ± 0.0003	1.30 ± 0.02	0.6819 ± 0.001	13.43

[a] Pressure uncertainty, ± 0.015 MPa.

5%, but the problem becomes more serious at the lower densities. For instance, for the benzene runs near 0.7 $g \cdot cm^{-3}$ (Nos. 3, 5–9), the spread of the diffusion coefficients exceeds 10%, and it is unlikely that the 2 K spread in temperature is the cause (see Section 4.3). As discussed before, we believe that part of the spread is due to differences in flow speed. As is clear from Fig. 2, however, there is considerable scatter even at constant flow speed. We conclude that there are still artifacts affecting the measurements, and the more seriously as the compressibility of the carrier fluid increases. In our apparatus, the limited stability of the expansion process is the most likely cause.

4.2. Other Taylor-Dispersion Data Sources for Benzene and Toluene in Carbon Dioxide

The review by Liong et al. [6] is a good source of information on data sources for benzene up to 1990. In addition to the data from Schneider and co-workers, they list the data of Sassiat et al. [31]. For toluene, Liong et al. show no data in our range. Since the appearance of that review, however, a number of new data sets have appeared. These include those of Umezawa and Nagashima [32] and of Erkey et al. [23] for benzene, those of Suárez and co-workers [33, 34] for benzene and toluene, and those of Bruno for toluene in carbon dioxide [22]. We give a few details on each of these experiments and then proceed to compare the data.

The Sassiat experiment shows the remarkable feature of a 10 m long dispersion tube that is straight. Although the absence of coiling is a highly desirable feature, it will be difficult to keep the temperature uniform over such a long length. The temperature constancy is reported to be ± 0.2°C. Sassiat et al. [31] work at the relatively high maximum pressure drop of 0.1 MPa and at a flow speed of 12 $mm \cdot s^{-1}$, according to Ref. 32. Sassiat et al. have spanned a very large range of densities, reaching all the way from liquid-like to gas-like densities. They have avoided the most serious effects of the high compressibility by measuring in the low-density range only at temperatures far from critical. At the 95% confidence level, their reported diffusion coefficients for benzene have uncertainties of the order of 2–4%. These authors have also examined the data with density as an independent variable and report the significant finding that at a density of 0.8 $g \cdot cm^{-3}$ the diffusion coefficient of benzene in carbon dioxide increases by only 7% over a temperature range of 30°C. At the density of 0.68 $g \cdot cm^{-3}$, there is no significant change of D_{12} over a range of 20°C.

Erkey et al. [23, 24] use a 9-m-long straight dispersion tube of 1-mm internal diameter, temperature-controlled to ± 0.2°C. A syringe pump and the use of two consecutive back pressure regulators assure flow constancy

to better than 0.2%. These authors have exerted much care in proving that the detector response is linear in concentration and have found it necessary to dilute their samples before injection, to at most 15% mole fraction of solute. They report some diffusion coefficients for benzene in carbon dioxide, but only in graphical form and as function of pressure. They claim an uncertainty of $\pm 5\%$.

In the experiment by Umezawa and Nagashima [32], the tube is also straight, but it is only 1 m long, with the temperature controlled to 0.1 K. The inner diameters in the cases of Sassiat et al., of Umezawa and Nagashima, and of our own experiment are all about 1 mm. The pressure drop, 0.6 Pa, and flow speed, $1\ \text{mm} \cdot \text{s}^{-1}$, in the experiment of Umezawa and Nagashima are much lower than in our case and in that of Sassiat et al., but because of the short tube, the Japanese experimenters can still carry out an entire experiment in a short time. Umezawa and Nagashima do not use an absorption detector. Instead, these authors observe the gradient of the refractive index at two positions along the tube and use this gradient as a measure of the concentration gradient. We have already estimated (Section 3.3) that in highly compressible states, there will be density gradients accompanying the concentration gradients. The relation between the refractive index and the solute concentration is nontrivial under such conditions and should, strictly speaking, be calibrated. Umezawa and Nagashima, however, have generally limited themselves to liquid-like densities where they find their data to agree with those of Sassiat et al. They claim an uncertainty of $\pm 3\%$ for the measured diffusion coefficients.

Suárez and co-workers, in a recent publication [33] and preprint [34], present a very useful and detailed overview of diffusion coefficients of many solutes in a variety of supercritical fluids. These articles also contain new data for several solutes in CO_2, including benzene and toluene. These authors use a commercial Hewlett–Packard chromatograph. The dispersion tube is 30 m long, has an inner radius of 0.38 mm, and is coiled with a diameter of 26 cm. The flow speed is $0.8\ \text{cm} \cdot \text{s}^{-1}$ or less.

Bruno [22] measured some diffusion coefficients of toluene in CO_2 at 313 K and various pressures as part of a wider study of applications of chromatography. He reports densities only, calculated from the pressure–temperature pairs by means of a BWR equation of state for carbon dioxide. Bruno predissolved the solute in the carrier gas at column conditions. The dispersion tube is a 30-m-long capillary coiled with a diameter of 30 cm, in order to fit in a commercial oven. The tube has a 0.25-mm inner diameter, only one-quarter of the size of those in the experiments discussed earlier. The flow speed is $2\text{–}6\ \text{cm} \cdot \text{s}^{-1}$ or below. Bruno achieves a temperature uniformity of ± 0.015 K, which is very good. He uses a flame ionization detector housed in a 300°C oven. This

instrument is linear over 8 decades of concentration and has an exceptional sensitivity. A quartz restrictor feeds the flowing gas directly into the flame. This eliminates some of the difficulties that come with a separate expansion section.

A difficult problem is that of detector linearity. For the data evaluation that follows, it is assumed that the detector signal is proportional to the solute concentration and that, consequently, the signal vs time data correspond to the concentration vs time history to a sufficient degree of approximation. Deviations from linearity, however, might exist even at very low concentrations for most of the detector types mentioned above. A careful calibration for detector linearity seems to be indispensable; up to now, such a calibration has been made only exceptionally.

4.3. Comparison of Diffusion Data for Benzene and Toluene in Carbon Dioxide

In the Taylor dispersion experiment, the diffusion coefficient is usually measured as a function of temperature and pressure. The steep dependence of fluid properties on pressure in the supercritical regime makes comparison of data awkward if not impossible. Matters simplify considerably when the comparison is made as a function of density. The paper by Sassiat et al. [31] gives some good guidance. As mentioned earlier, these authors find that the diffusion coefficient of benzene at a CO_2 density of $0.8\ g \cdot cm^{-3}$ increases no more than 10% over the temperature range of 303–333 K. These authors also show that at constant temperature the diffusion coefficient varies inversely with viscosity. This is consistent with the Stokes–Einstein concept that, at constant density, the mobility of a Brownian particle should vary linearly with temperature and be inversely proportional to the viscosity. At constant density, however, the viscosity of carbon dioxide is virtually independent of temperature in our range of interest [15, 31], so that over a range of 30 K, the diffusion coefficient should increase by approximately 10% at fixed density. The validity of the Stokes–Einstein relation has been discussed by many authors. We refer to the review by Liong et al. [6] for a thorough discussion. Variations on the Enskog theory for dense gases, such as the rough hard sphere theory, tested by Erkey et al. [23, 24], predict an even slower dependence of the diffusion coefficient on temperature, as $T^{1/2}$.

Different authors use different equations of state for CO_2 to convert pressure to density. Most equations of state are at their worst in the critical region. We have used the equation of Span and Wagner [14] that has been recently developed on the basis of highly accurate, as yet unpublished data. The differences with commonly used equations, such as the IUPAC

equation, may exceed 1% in density in some parts of the critical region. We will find that the uncertainties in the diffusion coefficient are so large that a 1% uncertainty in density is a minor source of error.

All the data for the diffusion coefficient of benzene in CO_2 are assembled as a function of density in one plot, Fig. 3. Because of insufficient resolution, it was not possible to convert and include the graphical D_{12} vs P data of Erkey et al. [23]. The following features are worth noting: The data from the Schneider group span a broad band of values; the Ellert and the Swidersky data are at the low end; and the Feist, some of the Swaid, and our own data are at the higher end. The spread is of the order of 15% in D_{12}. With the exception of the Swidersky and the Ellert data, all data sources agree within 10% for densities higher than 0.7 $g \cdot cm^{-3}$. Our new data reported here agree with those of Suárez et al. quite well. The data obtained with straight dispersion tubes, those of Sassiat et al. [31] and those of Umezawa and Nagashima [32], are consistently high, and the

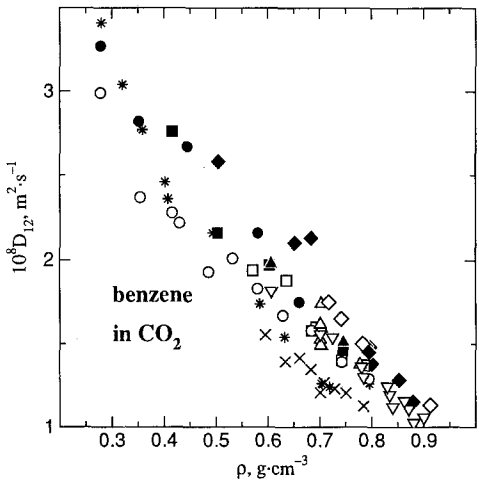

Fig. 3. Experimental diffusion coefficients of benzene in CO_2, grouped by authors. (■) Schneider and Swaid, 318.15–328.15 K, 11 MPa [16]; (□) Schneider and Swaid, 318.15–328.15 K, 13 MPa [16]; (○) Schneider and Swaid, 314.14 K, 8–16 MPa [16]; (●) Feist, 314.14 K, 8–16 MPa [28]; (*) Ellert, 312.99 K, 8–16 MPa [29]; (×) Swidersky, 314.14 K, 10–16 MPa [30]; (▲, △) this work, 307.92–314.14 K; (▽) Suárez, 313.15–333.15 K [34]; (◆) Sassiat et al., 303.15–333.15 K, 11–26.5 MPa [31]; (◇) Umezawa and Nagashima, 285.15–308.15 K, 10.5 MPa [32].

more so the lower the density. This is contrary to the expectation that tube coiling decreases the peak dispersion, thus apparently increasing the diffusion coefficient (Fig. 2). For densities below 0.7 $g \cdot cm^{-3}$, the disagreement between the various data sources quickly reaches 25%.

In order to explore temperature as a contributor to the variance, we show, in Fig. 4, the same data set coded by temperature range. There is little, if any, indication of systematics due to temperature differences. Bringing the 60°C data of Sassiat et al. [31] (filled squares in Fig. 4) down by 10% will certainly reduce the spread in Figs. 3 and 4, but it will do nothing to reduce the large spread in the 40°C data (crosses, Fig. 4), which also include data by Sassiat et al.

In Fig. 5, we collect all data for the diffusion coefficient of toluene in carbon dioxide. Again, our own data agree well with those of Suárez et al. [33, 34]. The data of Bruno have a much weaker density dependence than the other data. It is unlikely that this is due to the different equation of state used by Bruno, since his data are not in the highly compressible regime. In the case of benzene, the diffusion coefficient increases by roughly 50% between densities of 0.9 and 0.7 $g \cdot cm^{-3}$. In toluene, this increase is roughly of the same order for the same interval, according to our data. It is unlikely that the increase of barely 10% displayed by the Bruno data is correct.

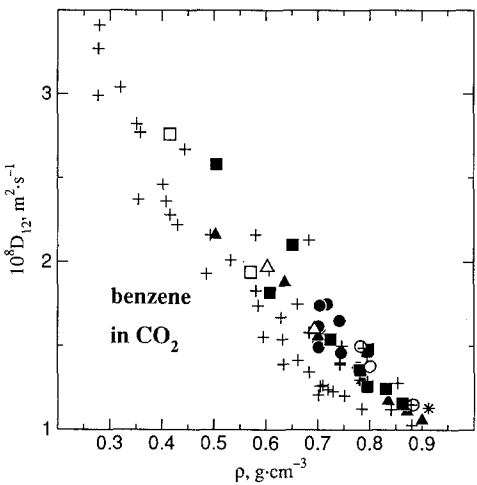

Fig. 4. Experimental diffusion coefficients of benzene in CO_2, grouped by temperatures. (*) 283–285 K; (○) 303 K; (●) 307–309 K; (+) 313–314 K; (△) 318 K; (▲) 323 K; (□) 328 K; (■) 333 K. For sources of data: see the legend to Fig. 3.

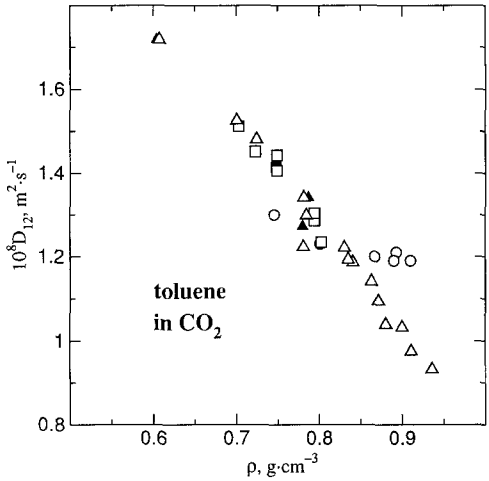

Fig. 5. Dependence of the diffusion coefficients of toluene in CO_2 on the density of CO_2. (○) Bruno, 313.82 K [22]; (■) this work, 313.74 K; (□) this work (modified apparatus), 306.12–308.36 K; (▲, △) Suárez, 313.15–333.15 K, 15–35 MPa [34].

There are several conclusions to be drawn from these intercomparisons. For densities exceeding $0.8\,g \cdot cm^{-3}$, the diffusion data for benzene in CO_2 generally agree to within 10%. The data at lower densities are beset with variations exceeding 25%. The data obtained with straight tubes are in mutual agreement with a maximum scatter of a few percent, but they are 10–30% higher than the data obtained in coiled tubes. The discrepancy between the coiled-tube and straight-tube results is of the opposite sign expected, since coiling leads to peak-sharpening (increased apparent D_{12}) under the present conditions (Fig. 2). The data for toluene in CO_2 show a basic disagreement in their density dependence. For applications in supercritical carbon dioxide around 40°C and below a density of $0.8\,g \cdot cm^{-3}$, the Taylor dispersion method, therefore, has not yet given results of proven reliability.

5. CRITICAL BEHAVIOR OF DIFFUSION COEFFICIENTS

5.1. Asymptotic Behavior

We first concern ourselves with the asymptotic critical behavior, that is, the behavior in a range so close to the critical point that the anomalous

critical behavior dominates to the extent that the normal background can be neglected. The characteristics of critical behavior are the strong divergence of the susceptibility (compressibility in pure fluids) and the related growth of the correlation length, a measure of the extent of a critical fluctuation. These divergences are described by means of power laws that indicate their strength along a specified path to the critical point. In pure fluids, this path is the critical isochore, $\rho = \rho_c$, in binary liquids the critical isopleth, $x = x_c$, and in gas–liquid systems near plait points it is a path with one density-like variable such as x or ρ held constant.

We then have the following power laws on this special path:

$$\text{susceptibility} \qquad \chi = \Gamma\,|\Delta T^*|^{-\gamma} \tag{12}$$

$$\text{correlation length} \qquad \xi = \xi_0\,|\Delta T^*|^{-\nu} \tag{13}$$

with

$$|\Delta T^*| = \frac{|T - T_c|}{T_c} \tag{14}$$

The exponent γ assumes the universal value of 1.24 and the exponent ν the value of 0.63 [35]. Γ and ξ_0 are critical amplitudes that vary from substance to substance. The mobility of a critical fluctuation asymptotically near a critical point is given by the Stokes–Einstein relation [36]

$$D = \frac{kT}{6\pi\eta\xi} \tag{15}$$

The viscosity of fluids and fluid mixtures has a very weak anomaly described by an exponent y which recently was definitively determined by Berg and Moldover [37] to have the value of 0.042. Thus

$$\eta = \eta_0\,|\Delta T^*|^{-y} \tag{16}$$

and the critical behavior of the mobility D, Eq. (15), is given by

$$D \sim |\Delta T^*|^{\nu + y} \tag{17}$$

which implies that D goes to zero with an exponent of $(\nu + y) = 0.67$ ("critical slowing down"). In a binary liquid mixture, D is identified with the diffusion coefficient D_{12}.

The mobility D goes to zero irrespective of whether the system is approaching a pure-fluid critical point, a plait point, or a consolute point. It is measured by correlation spectroscopy in dynamic light-scattering experiments [38–41]. The experiment of Chang et al. near the critical line

of CO_2–C_2H_6, for instance, vividly illustrates how the decay of the correlations in the mixtures smoothly interpolates between that of the pure components, without the possibility of distinguishing between composition and density fluctuations [41].

In a pure fluid, D is to be identified with the thermal diffusivity

$$D_T = \frac{\lambda}{\rho C_P} \tag{18}$$

with C_P the isobaric heat capacity (with a strong, γ-like divergence), and λ the thermal conductivity. Eqs. (12) and (17) imply that the thermal conductivity diverges according to

$$\lambda \sim |\Delta T^*|^{-(\gamma - \nu - y)} \tag{19}$$

The exponent has the value of 0.57, a little less than half the strength of the strong divergence of the susceptibility.

The thermal conductivity in a pure fluid is the heat flow resulting from a gradient in temperature, temperature being a "field" variable [42] equal in coexisting phases. In a fluid mixture, the so-called Onsager kinetic coefficient α is the flow of matter resulting from a spatial gradient in the chemical potential $\mu = \mu_2 - \mu_1$, again a field variable. These two coefficients λ and α have the same structure and the same critical behavior. Since the diffusion coefficient D_{12} is a flow of matter resulting from a spatial composition gradient, the relation between α and D_{12} is [43]

$$D_{12} = \frac{\alpha/\rho}{(\partial x/\partial \mu)_{P,T}} \tag{20}$$

so that the kinetic coefficient α behaves as

$$\alpha = \frac{kT\rho}{6\pi\eta\xi}\left(\frac{\partial x}{\partial \mu}\right)_{P,T} \tag{21}$$

and diverges with an exponent $-(\gamma - \nu - y)$, as the thermal conductivity in a pure fluid. The thermodynamic derivative $(\partial x/\partial \mu)_{P,T}$ is called the osmotic susceptibility. It is a strongly diverging quantity, just like the compressibility in a pure fluid.

5.2. Nonasymptotic Behavior

The relations of Section 5.1 are valid very near a critical point, when the critical divergences are dominating the scene. In reality, the asymptotic

equations are valid only for the critical part of the properties in question. Anisimov and Kiselev [43] as well as Mostert and Sengers [44] have worked out the nonasymptotic behavior of transport coefficients near plait points in binary mixtures. They stress that Eqs. (19) and (21) describe only the increase in the thermal conductivity or the Onsager kinetic coefficient over their respective background values. Taking the background part (with subscript b) explicitly into account in Eq. (21), we have

$$\alpha = \frac{kT\rho}{6\pi\eta\xi}\left(\frac{\partial x}{\partial \mu}\right)_{P,T} + \alpha_b \tag{22}$$

so that, with Eq. (20),

$$D_{12} = \frac{kT}{6\pi\eta\xi} + \frac{\alpha_b}{\rho}\left(\frac{\partial x}{\partial \mu}\right)^{-1}_{P,T} \tag{23}$$

Strictly speaking, the Stokes–Einstein term in Eq. (23) must be multiplied by a crossover function equal to 1 near a critical point and approaching the value 0 far away.

Anisimov and Kiselev now argue that, far from criticality, the second term has to provide the normal value of a diffusion coefficient. For a dilute mixture, $(\partial x/\partial \mu)^{-1}_{P,T}$ is dominated by the large ideal-mixing contribution RT/x, since x, the mole fraction of solute, is near 0. Therefore α_b has to be proportional to x for D_{12} to remain finite. A rough estimate of this far-away contribution may be obtained from the Stokes–Einstein relation

$$\frac{\alpha_b}{\rho}\left(\frac{\partial x}{\partial \mu}\right)^{-1}_{P,T} = \frac{kT}{6\pi\eta_b l} \tag{24}$$

with l indicating the size of the solute molecule and η_b the background viscosity.

When the mixture critical line is approached, the derivative $(\partial x/\partial \mu)^{-1}_{P,T}$, the inverse susceptibility, has to change its character profoundly, especially in dilute mixtures. From the value of RT/x, which is large for dilute mixtures, it has to go to the critical value of 0. As long as this derivative is not decreasing, the "critical slowing down" of the first term in Eq. (23) cannot be noticed, and the diffusion coefficient remains near its background value. The precise way in which the osmotic susceptibility changes from its dilute-mixture value to its critical value is a highly technical matter, worked out for dilute mixtures by Anisimov and co-workers [43] and by Chang and Levelt Sengers [45]. The essential point is that the osmotic susceptibility behaves as

$$\left(\frac{\partial x}{\partial \mu}\right)_{P,T} = x(1-x)[C_1 + x(1-x)\,|\Delta T^*|^{-\gamma}] \tag{25}$$

on the special path, and therefore, for small x, can become large only if

$$\Delta T^* \ll C_1^{-1/\gamma} x^{1/\gamma} \tag{26}$$

where the asymptotic constant C_1 depends on the initial slope of the critical line and other characteristics of the particular mixture under consideration. In a Taylor experiment carried out near infinite dilution, with x typically of the order of 10^{-4}, and with severe experimental restriction on closeness of approach, such as $|\Delta T^*| > 0.01$, this region can obviously not be entered, and only the nondiverging background value of the diffusion coefficient will be measured.

The only way the critical slowing down could be measured by Taylor dispersion is by carrying out the experiment with a binary mixture instead of a pure fluid as the carrier gas, similar to the experiment of Matos Lopes et al. [5] in a binary liquid mixture near a consolute point. This conclusion pertains as well to diffusion coefficients measured near infinite dilution by other techniques, such as tracer diffusion and NMR. In photon correlation spectroscopy, however, it is the mobility of the critical fluctuation, and its critical slowing down, that is measured [38–41]. Near infinite dilution, this property approaches the thermal diffusivity of the carrier gas and is, therefore, not a measure of the diffusion coefficient of the solute.

Since the Taylor dispersion experiment in the one-component carrier gas measures the nondiverging background of the diffusion coefficient, it may better be carried out in regions further from the critical point, where the experimental complications due to the high compressibility can be avoided.

6. SUMMARY

The challenges and difficulties of the application of the Taylor dispersion method for the measurement of diffusion coefficients in supercritical fluids have been exposed by concentrating on two systems, benzene and toluene in CO_2, for which we report new data and compare with all literature data available. The discrepancies between the different data sets are large (15–20% from the mean), in part unexplained. Contrary to theoretical expectation [13], straight tubes tend to yield higher diffusion coefficients than coiled tubes.

Although even D_{12} data of limited accuracy might already be useful for practical applications [e.g., in supercritical fluid technology for evaluating mass transfer in supercritical fluid extraction (SFE) or in supercritical fluid chromatography (SFC)], much smaller limits of error should be attainable

in high-precision experiments by careful consideration of all sources of error such as studied in this paper. This, however, would be a difficult task.

The large compressibility of the carrier fluid in the vicinity of its critical point amplifies the effects of variations of experimental variables such as pressure, temperature, and, especially, fluid composition; and it invalidates several of the assumptions made in the traditional analysis of the experiment, such as constancy of density. This excludes the applicability of the method in a region of at least 5 K from the critical point for densities within $\pm 50\%$ from the critical density. The theoretical understanding of the critical behavior of the diffusion coefficient near infinite dilution is that critical slowing down cannot be observed anyway in this density and temperature regime.

If diffusion coefficient information near infinite dilution is desired at densities in the general vicinity of the critical density, it is advisable to carry out Taylor dispersion measurements 20 K or more above the solvent's critical point.

ACKNOWLEDGMENTS

A Senior Scientist Award granted to one of us (J. M. H. Levelt Sengers) by the Alexander von Humboldt-Stiftung made it possible to carry out the work reported here. U. Dahlmann constructed the sample dilution loop, and both he and A. Kordikowski shared valuable experience with us. D. Rösener made major improvements in the principal thermostat. He, as well as R. Renzewitz and J. Masuch, provided expert assistance at various stages of the work. We thank A. Akgerman, T. J. Bruno, M. L. S. Matos Lopes, A. Nagashima, J. J. Suárez, J. L. Bueno de las Heras, W. A. Wakeham, and P. A. Wells for advice on the Taylor dispersion experiment, prepublication results, and discussions. We thank M. A. Anisimov, S. B. Kiselev, and J. V. Sengers for advice and discussions on the critical behavior of diffusion coefficients and H. R. van den Berg for prepublication results on flow profiles in highly compressible fluids. J. Lüttmer-Strathmann formed an essential link in the transatlantic transfer of manuscript drafts. R. Span and W. Wagner made their equation of state for CO_2 available to us before publication. R. F. Berg, T. J. Bruno, and R. F. Kayser served as careful readers.

REFERENCES

1. J. V. Sengers, *Critical Phenomena*, M. S. Green, ed. (Academic Press, New York, 1971), p. 466.
2. J. Kestin, J. H. Whitelaw, and T. F. Zien, *Physica* **30**:161 (1964).

3. A. Michels and J. V. Sengers, *Physica* **28**:1238 (1962).
4. A. Michels, J. V. Sengers, and P. S. van der Gulik, *Physica* **28**:1201, 1216 (1962).
5. M. L. S. Matos Lopes, C. A. Nieto de Castro, and J. V. Sengers, *Int. J. Thermophys.* **13**:283 (1992).
6. K. K. Liong, P. A. Wells, and N. R. Foster, *J. Supercrit. Fluids* **4**:91 (1991).
7. A. A. Clifford and S. E. Coleby, *Proc. Royal Soc. London A* **433**:63 (1991).
8. A. Alizadeh, C. A. Nieto de Castro, and W. Wakeham, *Int. J. Thermophys.* **1**:243 (1980).
9. G. I. Taylor, *Proc. Roy. Soc. A* **219**:186 (1953).
10. R. Aris, *Proc. Roy. Soc. A* **235**:67 (1956).
11. N. Dahmen, A. Kordikowski, and G. M. Schneider, *J. Chromatogr.* **505**:169 (1990).
12. L. A. M. Janssen, *Chem. Eng. Sci.* **31**:215 (1976).
13. R. J. Nunge, T. S. Lin, and W. N. Gill, *J. Fluid Mech.* **51**:363 (1972).
14. R. Span and W. Wagner, *J. Phys. Chem. Ref. Data.* (submitted).
15. V. Vesovic, W. A. Wakeham, G. A. Olchowy, J. V. Sengers, and J. T. R. Watson, *J. Phys. Chem. Ref. Data* **19**:763 (1990).
16. I. Swaid and G. M. Schneider, *Ber. Bunsenges. Phys. Chem.* **83**:969 (1979).
17. H. R. van den Berg, C. A. ten Seldam, and P. S. van der Gulik, *J. Fluid Mech.* **246**:1 (1993).
18. H. R. van den Berg, C. A. ten Seldam, and P. S. van der Gulik, *Int. J. Thermophys.* **14**:865 (1993).
19. J. M. H. Levelt Sengers, in *Supercritical Fluid Technology*, J. F. Ely and T. J. Bruno, eds. (CRC Press, Boca Raton, FL, 1991), p. 2.
20. J. M. H. Levelt Sengers, *J. Supercrit. Fluids* **4**:215 (1991).
21. H.-J. Ng and D. B. Robinson, *J. Chem. Eng. Data* **23**:325 (1978).
22. T. J. Bruno, *J. Res. NIST* **94**:105 (1989).
23. C. Erkey, H. Gadalla, and A. Akgerman, *J. Supercrit. Fluids* **3**:180 (1990).
24. A. Akgerman, private communication.
25. R. Feist and G. M. Schneider, *Sep. Sci. Technol.* **17**:261 (1982).
26. A. Wilsch, R. Feist, and G. M. Schneider, *Fluid Phase Equil.* **10**:299 (1983).
27. A. Kopner, A. Hamm, J. Ellert, R. Feist, and G. M. Schneider, *Chem. Eng. Sci.* **42**:2213 (1987).
28. R. Feist, Diploma thesis (Ruhr-Universität Bochum, 1980).
29. J. Ellert, Diploma thesis (Ruhr-Universität Bochum, 1986).
30. P. Swidersky, Diploma thesis (Ruhr-Universität Bochum, 1991).
31. P. R. Sassiat, P. Mourier, M. H. Caude, and R. H. Rosset, *Anal. Chem.* **59**:1164 (1987).
32. S. Umezawa and A. Nagashima, *J. Supercrit. Fluids* **5**:242 (1992).
33. J. J. Suárez, J. L. Bueno, I. Medina, and J. Dizy, *Afinidad* **IL**(438):101 (1992) (in Spanish).
34. J. J. Suárez and J. L. Bueno, *J. Chem. Eng. Data.* (in press).
35. J. V. Sengers and J. M. H. Levelt Sengers, *Annu. Rev. Phys. Chem.* **37**:189 (1986).
36. P. C. Hohenberg and B. I. Halperin, *Rev. Mod. Phys.* **49**:435 (1977).
37. R. F. Berg and M. R. Moldover, *Phys. Rev. A* **42**:7183 (1990).
38. D. L. Henry, L. E. Evans, and R. Kobayashi, *J. Chem. Phys.* **66**:1802 (1977).
39. B. J. Ackerson and H. J. M. Hanley, *J. Chem. Phys.* **73**:3568 (1980).
40. H. Saad and E. Gulari, *Ber. Bunsenges. Phys. Chem.* **88**:834 (1984).
41. R. F. Chang, T. Doiron, and I. L. Pegg, *Int. J. Thermophys.* **7**:295 (1986).
42. R. B. Griffiths and J. C. Wheeler, *Phys. Rev. A* **2**:1047 (1970).
43. M. A. Anisimov and S. B. Kiselev, *Int. J. Thermophys.* **13**:873 (1992).
44. R. Mostert and J. Sengers, *Fluid Phase Equil.* **76**:235 (1992).
45. R. F. Chang and J. M. H. Levelt Sengers, *J. Phys. Chem.* **90**:5921 (1986).